SAND2000-2995J

A GALERKIN IMPLEMENTATION OF THE GENERALIZED HELMHOLTZ DECOMPOSITION FOR VORTICITY FORMULATIONS

Marc S. Ingber[†] and Steven N. Kempka[‡]

[†] *Department of Mechanical Engineering, University of New Mexico Albuquerque, New Mexico 87131,* [‡] *Thermal/Fluid Computational Engineering Sciences Sandia National Laboratories Albuquerque, New Mexico 87185*

Vorticity formulations for the incompressible Navier-Stokes equations have certain advantages over primitive-variable formulations including the fact that the number of equations to be solved is reduced. However, the accurate implementation of the boundary conditions seems to continue to be an impediment to the acceptance and use of numerical methods based on vorticity formulations. Velocity boundary conditions can be implicitly satisfied by maintaining the kinematic compatibility of the velocity and vorticity fields as described by the generalized Helmholtz decomposition (GHD). This can be accomplished in one of two ways by either solving for boundary vorticity (leading to a Dirichlet boundary condition for the vorticity equation) or solving for boundary vortex sheet strengths (leading to a Neumann condition). In the past, vortex sheet strengths have often been determined by solving an over-specified set of linear equations. The over-specification arose because integral constraints were imposed on the vortex sheet strengths. These integral constraints are not necessary and typically are included to mitigate errors in determining the vortex sheet strengths themselves. Further, the constraints overspecify the linear system requiring least-squares solution techniques. To more accurately satisfy both components of the velocity boundary conditions, a Galerkin formulation is applied to the generalized Helmholtz decomposition. This formulation implicitly satisfies an integral constraint that is more general than many of the integral constraints that have been explicitly imposed. Two implementations of the Galerkin GHD are considered in the current work, one based on determining the boundary vorticity and one based on determining the boundary vortex sheet strengths. A finite element method (FEM) is implemented to solve the vorticity equation along with the boundary data generated from the GHD.

DISCLAIMER

Key Words: vorticity methods, generalized Helmholtz decomposition, Galerkin method

1. INTRODUCTION

Vorticity formulations of the incompressible Navier-Stokes equations have distinct advantages over velocity-pressure formulations. Some of these advantages include a reduction in the number of equations to be solved through the elimination of the pressure variable, identical satisfaction of the compressibility constraint and the continuity equation, an implicitly higher-order approximation of the velocity components, and, for exterior flow problems, a reduced computational domain. These advantages remain largely untapped, however, since questions concerning how to determine appropriate boundary conditions for vorticity formulations have not been fully resolved [21]. The problem is that the boundary conditions for the Navier-Stokes equations are typically given in terms of velocities, but boundary conditions in terms of vorticity are required for vorticity formulations. Thus, it is necessary to deduce vorticity boundary conditions from not only the velocity boundary conditions but also from the vorticity field in the domain. Vorticity boundary conditions can be given either in terms of prescribed vorticity or prescribed normal gradient (flux) of vorticity. The Navier-Stokes equations indicate that vorticity is created at the boundary in a way that satisfies the velocity boundary conditions [2]. However, neither the boundary vorticity nor its flux is generally known *a priori*, and hence, additional kinematic and, in the case of vorticity flux, dynamic equations must be introduced to relate boundary conditions to vorticity creation.

Many schemes to determine vorticity boundary conditions have been proposed comprising a wide range of different approaches. Approaches relying on kinematics include streamfunction-vorticity methods [26, 22, 24, 25, 1, 13], velocity-vorticity Cauchy methods [7], vorticity-velocity Poisson equation methods [5], Biot-Savart methods [4], and generalized Helmholtz decomposition (GHD) methods [29, 30, 31, 32, 18, 19, 28]. Other approaches are based on dynamics (Navier-Stokes equations) on the boundary [12, 33]. Several reviews have been written on this subject including those of Gresho [9], Puckett [23], Leonard [14, 15], and Sarpkaya [27].

Despite this large body of research, several questions concerning vorticity creation remain either unresolved or obscure. These questions include:

- Is there a unique specification of boundary vorticity or flux to satisfy velocity boundary conditions in each coordinate direction?
- Are integral constraints necessary when using the GHD to resolve vorticity created on the boundary and how can these constraints be implemented in a numerical algorithm?
- Should both normal and tangential components of the velocity boundary conditions be imposed or is it sufficient to impose only one component? If only one, which one?
- Are kinematics sufficient to specify vorticity flux creation or must dynamic information be used?
- Is the value of vorticity on the boundary (Dirichlet condition) or its normal derivative (Neumann condition) the appropriate boundary condition?

This paper discusses an approach which resolves many of these questions regarding vorticity boundary conditions.

Many of the above questions are interrelated. For example, the questions dealing with the unique specification of vorticity and imposition of integral constraints are related in that the integral constraint overspecifies the system of equations generated from the GHD. Hence, the solution may no longer be unique. Many investigators indicate that an overspecified set of equations must be solved to determine vorticity generation on the boundary including an integral constraint, although the precise mathematical justification for such constraints is not clear. For example, Wu [32] indicates that the linear system of equations based on a Helmholtz decomposition is rank deficient. For closure, Wu specifies that the volume integral of the vorticity field must be zero. Wu *et al.* [33] claim that a constraint is needed to exclude spurious solutions that arise because of the fact that the vorticity equation contains higher order derivatives of velocity. Sarpkaya [27] uses a constraint based on the requirement that the pressure be single-valued on the boundary. Koumoutsakos *et al.* [13] also indicate that an integral constraint is needed to obtain a unique solution; they use a constraint based on Kelvin's theorem. Quartapelle and

Valz-Gris [25] indicate that in order to satisfy both normal and tangential velocity boundary conditions for streamfunction-vorticity methods, vorticity created on the boundary must satisfy an *ad hoc* integral constraint.

The implementation of any integral constraint in addition to the GHD requires solving an overspecified system of linear equations. Further, at each point on the boundary, two components of vorticity or vorticity flux are unknown. Overspecification can also occur by attempting to determine the unknown vorticity components using velocity boundary conditions in all coordinate directions.

In this paper, an attempt is made to resolve many of the questions raised above. Vorticity creation either in terms of vortex sheet strengths or boundary vorticity can be accurately specified from purely kinematic considerations without the imposition of any integral constraints. However, in the case of vortex sheet strengths, dynamic considerations are required to relate the vortex sheet strengths to the vorticity flux at the boundary. Even though at each point along the boundary there are more components of specified velocity than unknown components of either the vortex sheet strengths or boundary vorticity, a unique specification of the vorticity flux or boundary vorticity exists that satisfies all components of the velocity boundary conditions.

Two approaches for determining vorticity boundary conditions are considered in this paper. Both are based on a Galerkin implementation of the generalized Helmholtz decomposition (GHD). In the first approach, the GHD is augmented to include the possibility of vortex sheets along the boundary. The vortex sheets are then related to the vorticity flux yielding Neumann boundary conditions for the vorticity equation. In the second approach, boundary vorticity is calculated directly from the GHD yielding Dirichlet boundary conditions. In both cases, it is shown that the normal component of the GHD yields a rank-deficient discretized system of equations whereas the tangential component implicitly satisfies an integral constraint. The Galerkin implementation of the GHD is shown to satisfy the velocity boundary conditions far better than the more common point-collocation methods.

The ultimate purpose of resolving the issues of accurate specification of the vorticity boundary conditions is to implement a method for determining these boundary conditions into a numerical algorithm based on the vorticity form of the Navier-Stokes equations. A Galerkin finite element method is presented for solving the vorticity equation. The accuracy of the formulation is demonstrated by considering the driven-lid cavity problem.

2. MATHEMATICAL FORMULATION

The vorticity form of the Navier-Stokes equations for an incompressible flow in two-dimensions is given by

$$\frac{\partial \vec{\omega}}{\partial t} + (\vec{u} \cdot \nabla)\vec{\omega} = \nu \nabla^2 \vec{\omega} \tag{1}$$

where $\vec{u}$ is the velocity field, $\vec{\omega} = \nabla \times \vec{u}$ is the vorticity field, t is time, ρ is the constant density field, and ν is the constant kinematic fluid viscosity. In the course of solving Eq. 1, the velocity field, $\vec{u}$, must be determined from the vorticity field, $\vec{\omega}$, and the creation of vorticity on the boundary must be determined from the velocity boundary conditions. In the present formulation, determining both the interior velocity field and the creation of vorticity on the boundary are accomplished in a unified manner using the generalized Helmholtz decomposition (GHD).

The GHD can be viewed as the infinite domain solution to the vector Poisson equation

$$\nabla^2 \vec{u} = -\nabla \times \vec{\omega} + \nabla D \tag{2}$$

obtained by performing the curl operation on the equation defining vorticity and identifying $D = \nabla \cdot \vec{u}$. In the present work, $D \equiv 0$ since only incompressible flows are considered. The GHD has been derived independently by several investigators including Wu and Thompson [29], Morino [18] (based on work by Bykhovskiy and Smirnov[3]), Uhlman and Grant [28] (based on work by Morse and Feshback [20]), and Meir and Schmidt [17]. It is interesting to note that none of these investigators reference one another except Morino who briefly notes some of Wu's work. A complete derivation of the GHD can be found in Kempka *et al.* [11].

The GHD for an incompressible fluid in two-dimensions is given by

$$\alpha(\vec{x})\vec{u}(\vec{x}) = \int_\Omega \frac{\vec{\omega}(\vec{y}) \times \vec{r}(\vec{x},\vec{y})}{r^2(\vec{x},\vec{y})} d\Omega(\vec{y}) + \int_\Gamma \frac{[\vec{u}(\vec{y}) \times \vec{n}(\vec{y})] \times \vec{r}(\vec{x},\vec{y})}{r^2(\vec{x},\vec{y})} d\Gamma(\vec{y}) - \int_\Gamma \frac{[\vec{u}(\vec{y}) \cdot \vec{n}(\vec{y})]\vec{r}(\vec{x},\vec{y})}{r^2(\vec{x},\vec{y})} d\Gamma(\vec{y}) \quad (3)$$

where $\vec{n}$ is the unit normal vector on the boundary (pointing away from the fluid), Ω represents the two-dimensional domain, and Γ is the boundary of Ω. The coefficient α is a function of the location of the field point $\vec{x}$. For field points outside of the domain, $\alpha = 0$; for field points in the interior of the domain, $\alpha = 2\pi$; for field points on smooth portions of the boundary, $\alpha = \pi$. At edges or corners, α can be related to a local internal angle. However, in the following development, a method is developed which circumvents having to evaluate α explicitly.

The GHD is valid only for certain kinematically admissible interior vorticity fields, $\vec{\omega}$, and velocity boundary conditions. For example, assume Eq. 3 is satisfied at a given time, τ, and consider an explicit time integration of the vorticity equation (Eq. 1). After the vorticity field has been transported but without properly taking into account the production and transport of vorticity at the boundary, Eq. 3 is no longer generally satisfied. There are essentially two ways that kinematic compatibility can be reestablished by satisfying the GHD.

Perhaps the most direct approach is to use the GHD to calculate updated values of the boundary vorticity [30, 10]. This leads to Dirichlet conditions for the vorticity equation. For two-dimensional problems, there are two components of the GHD but only one component of unknown vorticity. Wu [32] states that the normal and tangential component of the GHD are equivalent and either can be used to determine the boundary vorticity. In the following, it will be shown that, for Galerkin implementations, the normal component of the GHD leads to rank deficiency of the discretized linear system of equations. Despite the fact that the GHD represents a Fredholm equation of the first kind for the vorticity, the singular nature of the kernel function leads to a generally well-conditioned linear equation set.

A more subtle use of the GHD to reestablish kinematic compatibility is to represent the circulation associated with the newly created vorticity by a vortex sheet as proposed by Lighthill [16]. There is a jump in tangential velocity across the

vortex sheet equal to the strength of the sheet. On the fluid side of the sheet, the tangential velocity is specified while on the non-fluid side, the velocity is typically taken to be zero. Conveniently enough, the boundary integrals in Eq. 3 represent the motion induced by vortex sheets and source sheets with strengths $\vec{\gamma}$ and σ, respectively, given by

$$\vec{\gamma} = \vec{n} \times (\vec{u}_{nf} - \vec{u}) \text{ and } \sigma = \vec{n} \cdot (\vec{u}_{nf} - \vec{u}) \tag{4}$$

where, in the case of a stationary boundary, the non-fluid velocity $\vec{u}_{nf} = 0$ by definition. That is, the boundary integrals represent jumps in normal and tangential velocity on the boundary.

Circulation created on the boundary can be included by rewriting Eq. 3 to include the vortex sheet of strength $\vec{\gamma}$ as shown below

$$\begin{aligned} \alpha(\vec{x})[\vec{u}(\vec{x}) - \vec{\gamma}(\vec{x}) \times \vec{n}(\vec{x})] &= \int_{\Omega} \frac{\vec{\omega}(y) \times \vec{r}(\vec{x},\vec{y})}{r^2(\vec{x},\vec{y})} d\Omega(\vec{y}) \\ &+ \int_{\Gamma} \frac{[(\vec{u}(\vec{y}) - \vec{\gamma}(\vec{y}) \times \vec{n}(\vec{y})) \times \vec{n}(\vec{y})] \times \vec{r}(\vec{x},\vec{y})}{r^2(\vec{x},\vec{y})} d\Gamma(\vec{y}) \\ &- \int_{\Gamma} \frac{[\vec{u}(\vec{y}) \cdot \vec{n}(\vec{y})]\vec{r}(\vec{x},\vec{y})}{r^2(\vec{x},\vec{y})} d\Gamma(\vec{y}) \end{aligned} \tag{5}$$

By adding a vortex sheet along the boundary which accounts for the production of vorticity, the velocity boundary conditions can be satisfied after an explicit time step of the vorticity equation by exactly cancelling the induced slip velocity.

The solution of Eq. 5 yields the vortex sheet strengths, $\vec{\gamma}$, representing the creation of vorticity during a given time step. Although the determination of the vortex sheet strengths can be determined from purely kinematical considerations, the relationship between the vortex sheet strength and the flux of vorticity from the boundary into the domain depends on dynamics.

The definition of the vortex sheet, $\vec{\gamma}$, is given by

$$\vec{\gamma} = lim_{\omega \to \infty, dn \to 0} \vec{\omega}_{\tau} dn \tag{6}$$

The subscript τ in $\vec{\omega}_{\tau}$ indicates that the vorticity on the boundary must be in the tangential direction. In discreet form

$$\Delta\vec{\omega}_{\tau} = \vec{\gamma}/\Delta n \tag{7}$$

where Δn represents the distance over which the vorticity will diffuse in a time interval Δt. Integrating the vorticity equation over a small volume $V = A\Delta n$ and from t to $t + \Delta t$ yields

$$\int_t^{t+\delta t} \int_V \frac{D\vec{\omega}_\tau}{Dt} dV dt = \int_t^{t+\delta t} \int_V \nu \nabla^2 \vec{\omega}_\tau dV dt \tag{8}$$

At solid boundaries where vorticity is produced, the flow is parallel in the limit as $\Delta n \to 0$, and therefore, the convective flux of vorticity can be neglected in Eq. 8. Hence, using the divergence theorem

$$\int_t^{t+\delta t} \int_V \frac{\partial \vec{\omega}_\tau}{\partial t} dV dt = \int_t^{t+\delta t} \int_A \nu \frac{\partial \vec{\omega}_\tau}{\partial n} dA dt \tag{9}$$

This equation can be written in discrete form using a first-order approximation for the time derivative as

$$\Delta \vec{\omega}_\tau V = \nu \frac{\partial \vec{\omega}_\tau}{\partial n} A \Delta t \tag{10}$$

Hence, using Eq. 7, the following expression is obtained

$$\frac{\partial \vec{\omega}_\tau}{\partial n} = \frac{\vec{\gamma}}{\nu \Delta t} \tag{11}$$

That is, the vortex sheet strength can be related to the normal flux of vorticity on the boundary which can now be used as a Neumann boundary condition for the vorticity equation.

3. NUMERICAL IMPLEMENTATION

A Galerkin implementation of the GHD for determining either boundary vorticity or vortex sheet strengths is first presented in this section followed by some implementation issues associated with GHD. Next, a Galerkin finite element method (FEM) for solving the vorticity form of the Navier-Stokes equations is presented. Finally, an outline of the numerical algorithm for solving the vorticity equation is presented.

3.1. Galerkin Approximation of the GHD

One reason that may have been the cause of previous researchers imposing constraint equations on the GHD such as Stokes theorem is that the GHD itself was

poorly approximated. Excess vorticity created at each time step can accumulate in the interior of the flow domain causing a degradation of the solution over time. As shown in subsection 3.3, a Galerkin approximation of the GHD provides far more accurate results compared to the more popular point collocation methods.

A uniform approach can be taken to the discretization of either form of the GHD, that is, with or without vortex sheet strengths (see Eqs. 3 and 5). Let $\vec{v}$ represent either $\vec{u}$ or $\vec{u} - \vec{\gamma} \times \vec{n}$ depending on whether the Neumann (vortex sheet solution) or Dirichlet (boundary vorticity solution) formulation is desired. In either case, the GHD can be written as

$$\begin{aligned} \alpha(\vec{x})\vec{v}(\vec{x}) &= \int_{\Omega} \frac{\vec{\omega}(y) \times \vec{r}(\vec{x},\vec{y})}{r^2(\vec{x},\vec{y})} d\Omega(\vec{y}) + \int_{\Gamma} \frac{[\vec{v}(\vec{y}) \times \vec{n}(\vec{y})] \times \vec{r}(\vec{x},\vec{y})}{r^2(\vec{x},\vec{y})} d\Gamma(\vec{y}) \\ &- \int_{\Gamma} \frac{[\vec{v}(\vec{y}) \cdot \vec{n}(\vec{y})]\vec{r}(\vec{x},\vec{y})}{r^2(\vec{x},\vec{y})} d\Gamma(\vec{y}) \end{aligned} \tag{12}$$

The domain Ω is discretized into finite elements and the boundary of the domain Γ is discretized into boundary elements. Within the eth finite element, the jth component of $\vec{\omega}$ is approximated as

$$\omega_j^e(\vec{y}) = \sum_{l=1}^{4} \omega_{lj}^e S_l(\vec{y}) \tag{13}$$

where ω_{lj}^e represents the value of the jth component of $\vec{\omega}$ at the lth node within the eth finite element and S_l represents the biliniear Lagrangian shape function associated with the finite element. Similarly, within the eth boundary element, the jth component of $\vec{v}$ is approximated as

$$v_j^e(\vec{y}) = \sum_{l=1}^{2} v_{lj}^e N_l(\vec{y}) \tag{14}$$

where, in this case, v_{lj}^e represents the value of the jth component of $\vec{v}$ at the lth node within the eth boundary element and N_l represents the linear Lagrangian shape function associated with the boundary element. It is certainly possible to expand the boundary and finite element libraries without much difficulty but as seen in the results the linear boundary elements and bilinear finite elements provide excellent results.

Substituting Eqs. 13 and 14 into Eq. 12, the discretized form of the GHD can be written using indicial notation as

$$\alpha(\vec{x})v_i(\vec{x}) = \sum_{e=1}^{NFE}\int_{\Omega_e}\frac{e_{ijk}\omega_{lj}S_l(\vec{y})d_k}{d_r d_r}d\Omega + \sum_{e=1}^{NBE}\int_{\Gamma_e}\frac{e_{imp}e_{mjk}v_{lj}^e N_l(\vec{y})n_k d_p}{d_r d_r}d\Gamma - \sum_{e=1}^{NBE}\int_{\Gamma_e}\frac{v_{lj}^e N_l(\vec{y})n_j d_i}{d_r d_r}d\Gamma \tag{15}$$

where e_{ijk} is the unit alternating tensor, NFE represents the number of finite elements, NBE represents the number of boundary elements, and $d_i = x_i - y_i$ where $\vec{x} = (x_1, x_2)$ and $\vec{y} = (y_1, y_2)$.

Using the properties of the unit alternating tensor, this equation can be rewritten as

$$\alpha(\vec{x})v_i(\vec{x}) = \sum_{g=1}^{NFE}\int_{\Omega_g}\frac{e_{ijk}\omega_{lj}^g S_l d_k}{d_r d_r}d\Omega + \sum_{e=1}^{NBE}\int_{\Gamma_e}\frac{v_{lk}^e N_l d_k n_i - v_{li}^e N_l d_k n_k - v_{lk}^e N_l d_i n_k}{d_r d_r}d\Gamma. \tag{16}$$

It is possible at this point to multiply the above equation by the nodal basis functions associated with the boundary element shape functions N_l and perform a second integral over the boundary Γ in order to determine a Galerkin approximation of the GHD. However, a single integral would result on the right hand side of the equation whereas a double integral would result on the left hand side of the equation. This is cumbersome, both from a programming and a bookkeeping point of view.

The term $\alpha(\vec{x})v_i(\vec{x})$ can be incorporated directly into the boundary integral by considering rigid body arguments [6]. That is, if v_i is constant, then the associated vorticity field is identically zero. Hence,

$$\alpha(\vec{x})v_1 = -v_1\int_\Gamma\frac{d_k n_k}{d_r d_r}d\Gamma + v_2\int_\Gamma\frac{d_2 n_1 - d_1 n_2}{d_r d_r}d\Gamma \tag{17}$$

$$\alpha(\vec{x})v_2 = -v_2\int_\Gamma\frac{d_k n_k}{d_r d_r}d\Gamma - v_1\int_\Gamma\frac{d_2 n_1 - d_1 n_2}{d_r d_r}d\Gamma \tag{18}$$

Consider the terms

$$\int_\Gamma\frac{d_2 n_1 - d_1 n_2}{d_r d_r}d\Gamma = \int_\Gamma\vec{w}\cdot\vec{n}d\Gamma \tag{19}$$

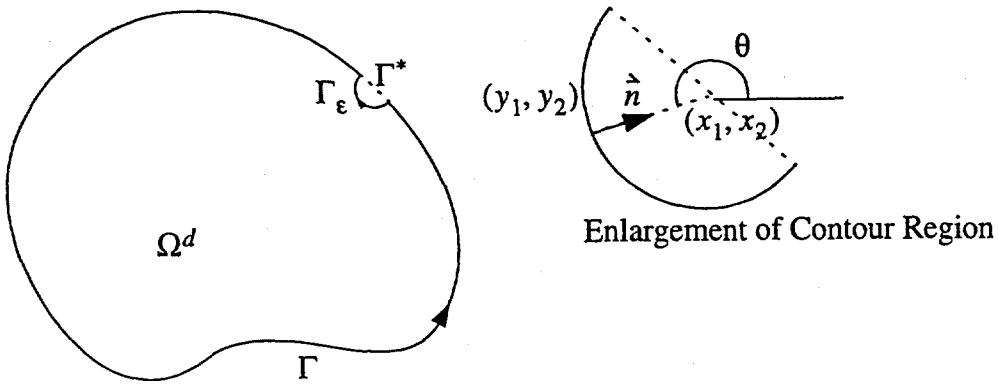

FIG. 1. Deformation of the domain Ω to exclude the field point $\vec{x} = (x_1, x_2)$. The deformed domain Ω^d has boundary $\Gamma - \Gamma^* + \Gamma_\epsilon$.

As shown in Figure 1 on Γ_ϵ, $d_2/\sqrt{d_r d_r} = -\sin\theta$, $d_1/\sqrt{d_r d_r} = -\cos\theta$, $n_1 = -\cos\theta$, and $n_2 = -\sin\theta$. Hence,

$$\int_{\Gamma_\epsilon} \frac{d_2 n_1 - d_1 n_2}{d_r d_r} d\Gamma = \int_{\Gamma_\epsilon} \frac{\sin\theta\cos\theta - \cos\theta\sin\theta}{\sqrt{d_r d_r}} d\Gamma = 0 \tag{21}$$

In the limit as $\epsilon \to 0$, $\Gamma - \Gamma^* \to \Gamma$, and hence

$$\int_{\Gamma} \frac{d_2 n_1 - d_1 n_2}{d_r d_r} d\Gamma = 0 \tag{22}$$

Therefore, inserting Eq. 22 into either Eq. 17 or Eq. 18 yields

$$\alpha(\vec{x}) = -\int_{\Gamma} \frac{d_k n_k}{d_r d_r} d\Gamma \tag{23}$$

Using Eqs. 22 and 23, the left hand side of Eq. 16 can be incorporated into the right hand side. The resulting integral equation is given by

$$0 = \sum_{g=1}^{NFE} \int_{\Omega_g} \frac{e_{ijk}\omega_{lj}^g S_l(\vec{y}) d_k}{d_r d_r} d\Omega + \sum_{e=1}^{NBE} \int_{\Gamma_e} \frac{[v_{lk}^e N_l(\vec{y}) - v_i(\vec{x})](d_k n_i - d_i n_k) - [v_{li}^e N_l(\vec{y}) - v_i(\vec{x})] d_k n_k}{d_r d_r} d\Gamma \tag{24}$$

This formulation not only has the advantage of not having to evaluate $\alpha(\vec{x})$ explicitly, but also regularizes the Cauchy Principal Value integral on the right hand side of Eq. 16.

Now to obtain a Galerkin approximation, Eq. 23 is multiplied by the shape functions $N_m(\vec{x})$ and integrated over the the boundary Γ. Assuming that $N_m(x)$ has support within the fth boundary element and within that element

$$v_k(\vec{x}) \mid_{\Gamma_f} = v_{lk}^f N_l(\vec{x})$$

the discretized Galerkin approximation for the GHD is given by

$$0 = \sum_{g=1}^{NFE} \int_{\Gamma_f} N_m(\vec{x}) \int_{\Omega_g} \frac{e_{ijk}\omega_{lj}^g S_l(\vec{y}) d_k}{d_r d_r} d\Omega + \sum_{e=1}^{NBE} \int_{\Gamma_f} N_m(\vec{x}) \int_{\Gamma_e} \frac{[v_{lk}^e N_l(\vec{y}) - v_{li}^f N_l(\vec{x})](d_k n_i - d_i n_k)}{d_r d_r} d\Gamma - \sum_{e=1}^{NBE} \int_{\Gamma_f} N_m(\vec{x}) \int_{\Gamma_e} \frac{[v_{li}^e N_l(\vec{y}) - v_{li}^f N_l(\vec{x})] d_k n_k}{d_r d_r} d\Gamma \tag{25}$$

3.2. Implementation Issues for the Solution of the GHD

There is some bookkeeping associated with the implementation of Eq. 25 for solving for either the boundary vorticity or the vortex sheet strengths. In the case of solving for the boundary vorticity, the interior nodal values of vorticity get assembled as part of the load vector whereas the boundary nodal values of vorticity represent the unknown vector. In the case of solving for the vortex sheet strengths, the vector $\vec{v}$ is comprised of both known values of $\vec{u}$ and unknown values of $\vec{\gamma}$.

Beyond the improvement in satisfying the velocity boundary conditions afforded by the Galerkin implementation of the GHD as shown in the following subsection, there is a conceptual advantage as well. As discussed in Section 2, the discretized normal and tangential components of the GHD represent $2N$ equations in N unknowns where N is the number of degrees of freedom used to represent the boundary vorticity or vortex sheet strengths in discrete form. There have been questions in the past concerning which component of the GHD (if either) is more appropriate for solving for the unknown source densities.

First, consider the formulation to determine Neumann conditions by solving for the vortex sheet strengths in the GHD. Starting from Eq. 16, a discretized form of the Galerkin GHD double integral can be written as

$$\int_{\Gamma_f} N_m(x)\alpha(\vec{x})v_{li}^f(\vec{x})N_l d\Gamma(\vec{x}) = \sum_{g=1}^{NFE}\int_{\Gamma_f} N_m(x)\int_{\Omega_g}\frac{e_{ijk}\omega_{ij}^g S_l d_k}{d_r d_r}d\Omega(\vec{y})d\Gamma(\vec{x}) + \sum_{e=1}^{NBE}\int_{\Gamma_f} N_m(x)\int_{\Gamma_e}\frac{v_{lk}^e N_l d_k n_i - v_{li}^e N_l d_k n_k - v_{lk}^e N_l d_i n_k}{d_r d_r}d\Gamma(\vec{y})d\Gamma(\vec{x}) \quad (26)$$

Since $N_1(x) + N_2(x) = 1$ for any element, the column sum (*col. sum*) of the discretized equations to solve for the unknown vortex sheet strengths using either the tangential or normal component of the GHD is given by

$$\begin{aligned} col.\ sum \ = \ & \int_{\Gamma_s}\alpha(\vec{x})p_i^f(\vec{x})N^s(\vec{x})q_i(\vec{x})\Gamma(\vec{x}) \\ & - \int_{\Gamma_s}\int_{\Gamma}\frac{p_k^e(\vec{y})N^s(\vec{y})q_i(\vec{x})(d_k n_i(\vec{y}) - d_i n_k(\vec{y}))}{d_r d_r}d\Gamma(\vec{x})d\Gamma(\vec{y}) \\ & + \int_{\Gamma_s}\int_{\Gamma}\frac{p_i^e(\vec{y})N^s(\vec{y})}{d_r d_r}d\Gamma(\vec{x})d\Gamma(\vec{y}) \end{aligned} \quad (27)$$

where p_i^e represents the ith component of the vector $\vec{p} = (-n_2, n_1)$ within the eth element, $N^s(\vec{y})$ is the nodal basis function comprised on $N_2(\vec{y})$ from the element on the left and $N_1(\vec{y})$ from the element on the right, Γ_s is the support of the nodal basis function, and the vector $\vec{q} = (q_1, q_2)$ represents either $\vec{n}$ or $\vec{t}$ depending on whether the normal or tangential component of the GHD is desired. That is, taking a column sum of the discretized equations is essentially equivalent to choosing two adjacent Γ_f's in the inner integration in Eq. 26 and integrating over the entire boundary in the outer integral (although the order of integration is interchanged in Eq. 27).

Since it has been shown that

$$\int_\Gamma \frac{d_2 n_1(\vec{x}) - d_1 n_2(\vec{x})}{d_r d_r} d\Gamma(\vec{x}) = 0$$

and

$$\int_\Gamma \frac{d_k n_k(\vec{x})}{d_r d_r} d\Gamma(\vec{x}) = \alpha(\vec{y}),$$

choosing $\vec{q} = \vec{n}$ yields

$$col.\ sum = 2 \int_{\Gamma_s} \alpha(\vec{y}) N^s(\vec{y}) p_i(\vec{y}) n_i(\vec{y}) d\Gamma(\vec{y}) = 0 \tag{28}$$

since $\vec{p}$ is perpendicular to $\vec{n}$. On the other hand, choosing $\vec{q} = \vec{t}$ yields

$$\begin{aligned} col.sum &= 2 \int_{\Gamma_s} \alpha(\vec{y}) N^s(\vec{y}) [(p_2(\vec{y}) n_1(\vec{y}) - p_1(\vec{y}) n_2(\vec{y})] d\Gamma(\vec{x}) \\ &= 2 \int_{\Gamma_s} \alpha(\vec{y}) N^s(\vec{y}) d\Gamma(\vec{y}) \end{aligned} \tag{29}$$

These results can also be interpreted physically. The column sum can be related to the integral over the boundary of the component of velocity corresponding to $\vec{q}$ induced by a vortex sheet within Γ_s. For the normal component of velocity, this integral over the boundary can be related to the integral over the domain of the divergence of the induced velocity by the divergence theorem. However, the integral of the divergence of the induced velocity over the domain must be zero since the flow field is incompressible. Similarly, for the tangential component of the velocity, the integral of the tangential velocity over Γ is related to the induced vorticity over the domain by Stokes theorem which is nonzero.

Next, consider the formulation to determine Dirichlet boundary conditions by solving for the boundary vorticity in the the GHD. Again, since $N_1(x) + N_2(x) = 1$ for any element, the column sum of the discretized equations to solve for the unknown boundary vorticity using either component of the GHD is given by

$$col.\ sum = \int_{\Omega_s} \int_\Gamma \frac{S^s(\vec{y})(d_1 q_2(\vec{x}) - d_2 q_1(\vec{x}))}{d_r d_r} d\Gamma(\vec{x}) d\Omega(\vec{y}) \tag{30}$$

where Ω_s is the support of the nodal basis function S^s. This nodal basis function is typically the union of two of the bilinear shape functions from adjacent finite

elements except for in corners of the domain. Choosing $\vec{q} = \vec{n}$, the column sum is again seen to be zero from Eq. 22. Choosing $\vec{q} = \vec{t}$ and using Eq. 23, the column sum is given by

$$col.\ sum = \int_{\Omega_s} \alpha(\vec{y}) S^s(\vec{y}) d\Omega_c \tag{31}$$

This analysis shows that, for either formulation (i.e., determining boundary vorticity or vortex sheet strengths), the normal component of the GHD yields rank-deficient linear systems. In either case, the accuracy of the numerical quadratures can be evaluated since the integrals in Eqs. 29 and 31 are easy to evaluate analytically and can be compared to the column sums resulting from the discretized GHD. However, there is an important difference between Eqs. 29 and 31. In the case of Eq. 29, $\alpha(\vec{y}) = \pi$ almost everywhere since the outer integral in Eq. 27 is over a portion of the boundary. On the other hand in the case of Eq. 31, $\alpha(\vec{y}) = 2\pi$ almost everywhere since the outer integral in Eq. 27 is over a portion of the domain. Actual column sums are performed in Section 4 to show the accuracy of the numerical integrations in the current implementation.

3.3. Accuracy Assessment of the Galerkin GHD

A simple benchmark problem is considered to show the improvement in the numerical results for the vortex sheet strengths using the Galerkin implementation of the GHD compared to the results using the more traditional point-collocation implementation. The benchmark problem consists of a uniform field of unit vorticity in the unit square. The normal and tangential velocity components on one side of the unit square induced by the unit vorticity is shown in Figure 2. The objective of this benchmark problem is to solve for the vortex sheet strengths on the boundary that cancel out the induced components of velocity to essentially yield no-slip boundary conditions. Recall that, analytically, if the tangential component of the velocity boundary condition is satisfied by the GHD, then the normal component must also be satisfied. In discrete systems, however, the tangential component of velocity is not identically satisfied exactly, and hence, neither is the normal component. Nevertheless, errors in both components are shown to decrease with increasing grid resolution.

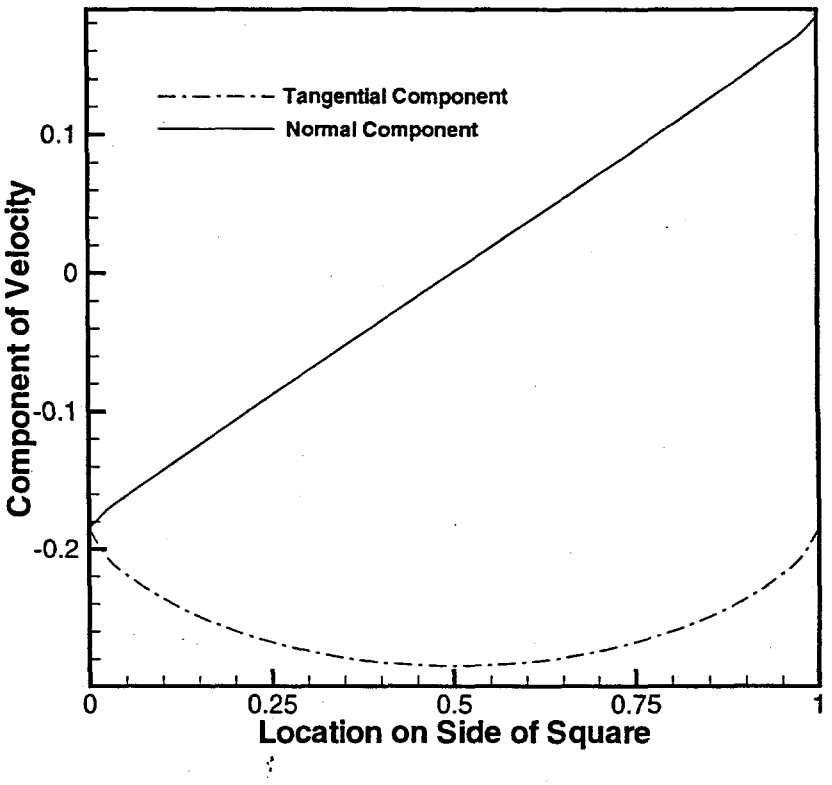

FIG. 2. Induced normal and tangential velocity for the unit vorticity in unit square problem.

The vortex sheet strengths as calculated by the Galerkin and point-collocation implementations of the GHD are shown in Figure 3. As seen in the Figure, the Galerkin results using 20 and 100 elements per side are visually indistinguishable. The results generated using the point-collocation method are seen to to oscillate about the Galerkin results.

Possibly more important than the accuracy of the vortex sheet solution is how well the no-slip boundary conditions are satisfied by the calculated vortex sheet strengths. The absolute value of the tangential component of velocity computed along one half of the side of the unit square is shown in Figure 4. The velocity calculations are performed in postprocessing using the calculated values of the vortex sheet strengths shown in Figure 3. As seen in the Figure, the Galerkin implementation of the GHD yields errors that are over 2 orders of magnitude smaller than

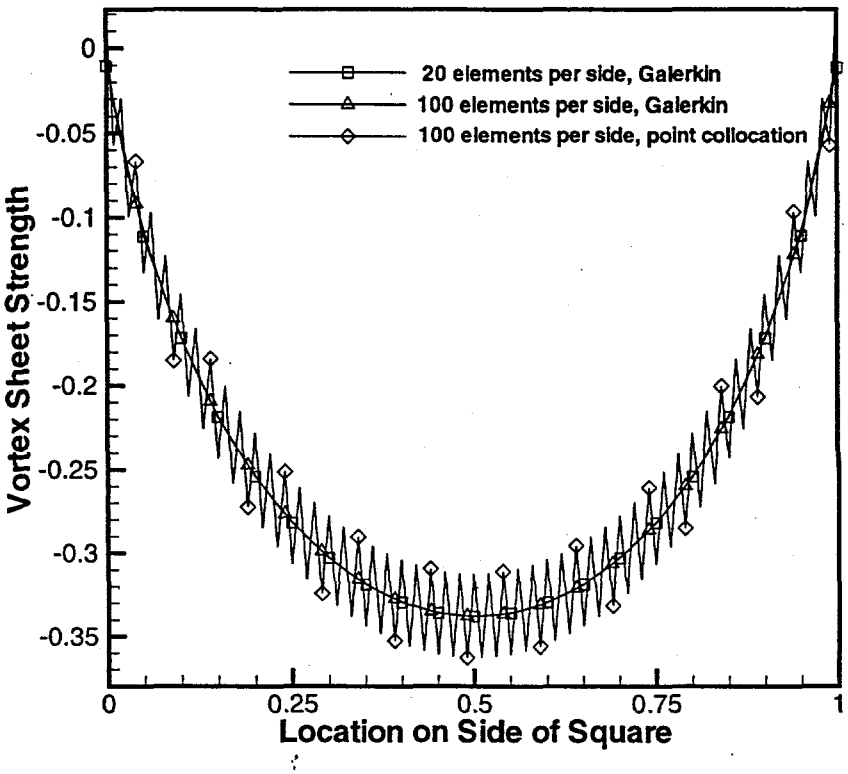

FIG. 3. Vortex sheet strengths calculated for the uniform vorticity in unit square problem.

the point-collocation implementation for the same discretization. In fact, the errors using a Galerkin implementation and 20 linear elements per side yields far better solutions than the point-collocation formulation using 100 linear elements per side. Similar results are shown for the normal component of velocity in Figure 5. Again, the boundary condition in the normal direction is satisfied far better using the Galerkin method compared to the point-collocation method. It is interesting to note that the magnitude of error for the normal component of velocity is almost the same as for the tangential component even though the actual condition imposed numerically was for the tangential component. In fact, for the Galerkin implementation using 100 elements per side, it appears that the normal velocity condition is satisfied slightly better than the tangential component.

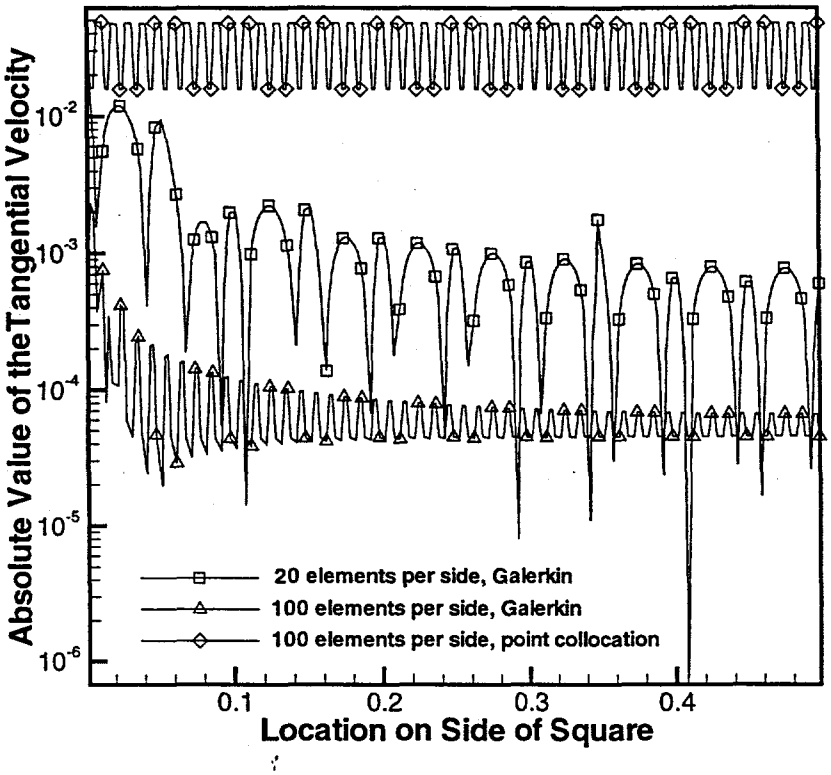

FIG. 4. Absolute value of the tangential component of velocity along one half side of the unit square. Note, zero is the prescribed value.

3.4. Galerkin FEM Solution of the Vorticity Equation

The Galerkin finite element method used to solve the vorticity equation is outlined in this subsection. Multiplying the 2D vorticity equation (Eq. 1) by a weighting function, w, and integrating over the domain yields

$$\int_\Omega w\frac{\partial\omega}{\partial t}d\Omega + \int_\Omega \left[u_x w\frac{\partial\omega}{\partial x} + u_y w\frac{\partial\omega}{\partial y}\right] d\Omega - \int_\Omega \left[+\nu w\frac{\partial^2\omega}{\partial x^2} + \nu w\frac{\partial^2\omega}{\partial y^2}\right] d\Omega = 0 \quad (32)$$

where u_x and u_y are the components of the velocity vector $\vec{u}$. Integrating the second-order terms by parts (applying Green's theorem), the weak form of the vorticity equation is written as

$$\int_\Omega w\frac{\partial\omega}{\partial t}d\Omega + \int_\Omega \left(u_x w\frac{\partial\omega}{\partial x} + u_y w\frac{\partial\omega}{\partial y}\right) d\Omega + \int_\Omega \nu\left(\frac{\partial\omega}{\partial x}\frac{\partial w}{\partial x} + \frac{\partial\omega}{\partial y}\frac{\partial w}{\partial y}\right) d\Omega = \int_{\Gamma_n} w q_n d\Gamma \quad (33)$$

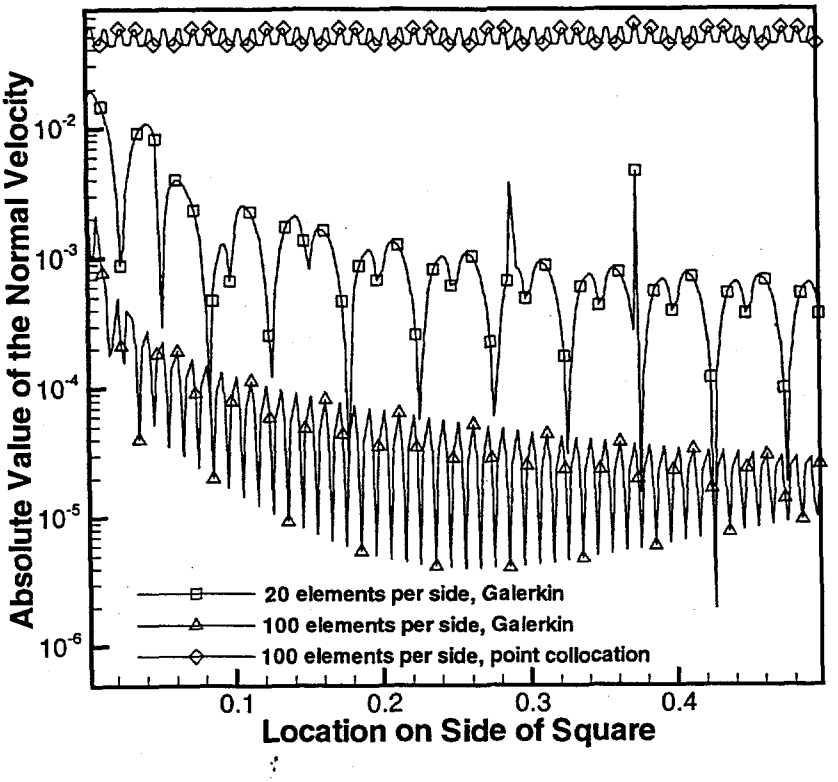

FIG. 5. Absolute value of the normal component of velocity along one half side of the unit square. Note, zero is the prescribed value.

where Γ_n is the portion of the boundary where Neumann conditions are prescribed and the flux q_n is defined by

$$q_n = \nu(\vec{n} \cdot \nabla)\vec{\omega} \tag{34}$$

For Neumann problems, $\Gamma_n = \Gamma$ and using Eq. 11, the vorticity flux is given in terms of the vortex sheet strengths as

$$q_n = \frac{\gamma}{\Delta t} \tag{35}$$

For Dirichlet problems, the boundary vorticity is calculated directed from the GHD assuming all vortex sheet strengths are zero.

The weak form of the vorticity equation is discretized by subdividing the domain Ω into finite elements and subdividing the boundary Γ into boundary elements. Using isoparametric bilinear Lagrangian interpolation for the finite elements and

linear interpolation for the boundary elements, the weak form of the vorticity equation can be written in discrete form as

$$\sum_{i=1}^{nbe} w_i^e \int_{\Gamma_e} N_i^e \frac{N_k^e}{\Delta t} d\Gamma \gamma_k^e = \sum_{e=1}^{nfe} w_i^e \int_{\Omega^e} S_i S_j d\Omega \frac{d\omega_j^e}{dt} + \sum_{e=1}^{nfe} \left(w_i^e \nu \int_{\Omega_e} \frac{\partial S_i}{\partial x}\frac{\partial S_j}{\partial x} + \frac{\partial S_i}{\partial y}\frac{\partial S_j}{\partial y} d\Omega \right) \omega_j^e + \sum_{e=1}^{nfe} \left(w_i^e \int_{\Omega_e} S_i \frac{\partial S_j}{\partial x} u_{xk}^e S_k + S_i \frac{\partial S_j}{\partial y} u_{yk}^e S_k \right) d\Omega \omega_j^e \tag{36}$$

where nfe is the number of finite elements, nbe is the number of boundary elements, w_i^e, ω_i^e, u_{xi}^e, u_{yi}^e represent the value of w, ω, u_x, and u_y, respectively, at the ith node within the eth finite element, S_i represents the bilinear finite element shape function, γ_i^e represents the value of γ at the ith node within the eth boundary element, and N_i represents the linear boundary element shape function.

For convenience, the element capacitance matrices, element stiffness matrices, and element load vectors are defined by

$$(C^e)_{ij} = \int_{\Omega_e} S_i^e S_j^e d\Omega \tag{37}$$

$$(K_x^e)_{ij} = \nu \int_{\Omega_e} \frac{\partial S_i^e}{\partial x}\frac{\partial S_j^e}{\partial x} d\Omega \tag{38}$$

$$(K_y^e)_{ij} = \nu \int_{\Omega_e} \frac{\partial S_i^e}{\partial y}\frac{\partial S_j^e}{\partial y} d\Omega \tag{39}$$

$$(K_u^e)_{ij} = \sum_{k=1}^{4} u_{xk}^e \int_{\Omega_e} S_i^e \frac{\partial S_j^e}{\partial x} S_k^e d\Omega \tag{40}$$

$$(K_v^e)_{ij} = \sum_{k=1}^{4} u_{yk}^e \int_{\Omega_e} S_i^e \frac{\partial S_j^e}{\partial y} S_k^e d\Omega \tag{41}$$

$$(F^e)_i = \frac{1}{\Delta t} \gamma_k^e \int_{\Gamma_e} N_i^e N_j^e d\Gamma \tag{42}$$

The discretized weak form can now be written in the following convenient form

$$\sum_{e=1}^{nfe} w_i^e (C^e)_{ij} \dot{\omega}_j^e + \sum_{e=1}^{nfe} w_i^e \left\{ (K_x^e)_{ij} + (K_y^e)_{ij} + (K_u^e)_{ij} + (K_v^e)_{ij} \right\} \omega_j^e = \sum_{e=1}^{nbe} w_i^e (F^e)_i \tag{43}$$

After assembly and dividing through by the Galerkin vector $\{w\}$, the assembled finite element equations become

$$[K_x + K_y + K_u + K_v]\{\omega\} + [C]\{\dot{\omega}\} = \{F\} \tag{44}$$

The discretized equation set (Eq. 44) is inherently nonlinear since the matrices K_u and K_v contain the unknown velocity field components. In the current implementation, the velocity components in K_u and K_v are evaluated using Eq. 3 for the Dirichlet problem or Eq. 5 for the Neumann problem to evaluate the velocity components. Time is discretized using an Euler explicit integrator which is first-order accurate in time.

3.5. Outline of the Numerical Algorithm

The numerical algorithm for solving the vorticity form of the Navier-Stokes equations is briefly outlined in this subsection. First, the vortex sheet strengths or boundary vorticity is calculated using the tangential component of the Galerkin form of the GHD (Eq. 25) to determine either Neumann or Dirichlet boundary conditions for the vorticity equation. Next, the internal velocities at the finite element interior nodes are evaluated using the regular form of the GHD (either Eq. 3 or 5). Finally to complete the time step, the vorticity field is transported by solving the explicit form of the finite element equations. After the explicit convection of vorticity, the flow field is again kinematically incompatible without incorporating newly formed vorticity or vortex sheet strengths at the boundary. This kinematic incompatibility is resolved by going back to the first step.

In the current implementation of the numerical algorithm, both the discretized FEM equations and discretized GHD equations are solved using an LU solver. The decomposition is done outside the time loop. Further, all integrals for evaluating the interior velocities are also performed outside the time loop. Hence, within the time loop, the majority of calculation is matrix-vector multiplication and backwards substitution.

4. NUMERICAL EXAMPLE

The impulsively-started driven square cavity problem at a Reynolds number of 400 is considered to demonstrate the reliability and accuracy of the overall algorithm. This example is difficult numerically because of the discontinuous boundary conditions where the top lid meets the sidewalls and because of the discontinuity between initial and boundary conditions. For a unit cavity, steady state is achieved in approximately 40 seconds. The current results are generated using a constant time step of 0.001, 1600 finite elements, and 160 boundary elements (41x41 grid). The measured CPU time for all calculations outside of the time loop was 93.4 seconds. The CPU time per time step within the loop was 2.9 seconds showing the efficiency of the current approach for running through the transient.

The streamline pattern and vorticity field generated using the current formulation with Neumann boundary conditions, (that is, solving for the vortex sheet strengths), are shown in Figures 6 and 7.

The velocity and vorticity fields are essentially the same at steady state for both the Dirichlet and Neumann vorticity formulations since, at steady state, the GHD should be satisfied after an explicit step in the vorticity equation without any vortex sheets. The results shown in Figures 6 and 7 qualitatively look the same as the results generated by Ghia, Ghia, and Shen [8] who used a multigrid finite difference method (FDM) on a 129x129 grid.

To demonstrate the agreement between the current results and the multigrid results, calculated values for the u-component of velocity along the vertical line through the geometric center of the cavity is shown in Figure 8. Five sets of numerical results are shown in the Figure. The results generated using the Dirichlet and Neumann vorticity formulations on a 41x41 grid are visually indistinguishable from the results generated by the multigrid finite difference method on a 129x129 grid. The convergence of the Dirichlet vorticity formation can be seen qualitatively by viewing the 21x21 grid and 41x41 grid results. Finer discretizations for the vorticity formulations produce results which are indistinguishable from the 41x41 grid results. Finally, results generated by a primitive-variables FEM code using 400 bi-quadratic 9-node quadrilateral elements is also shown. The primitive-variable

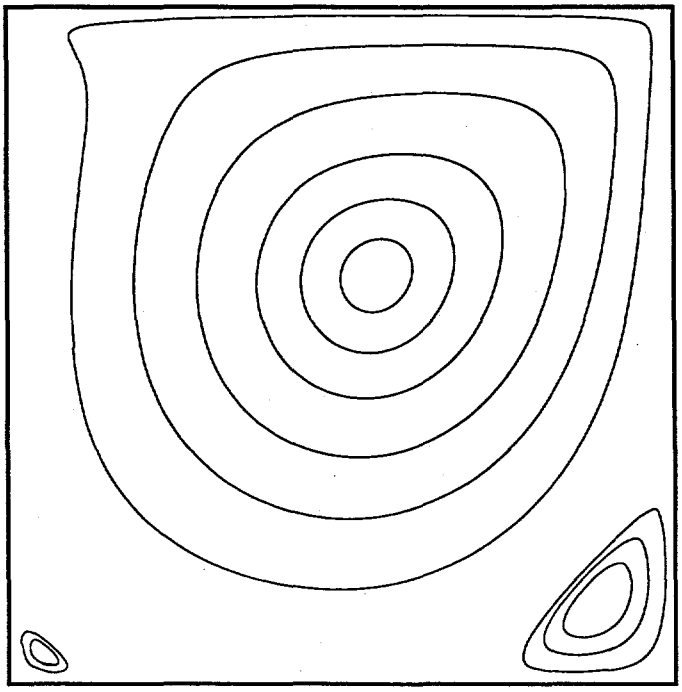

FIG. 6. Streamline pattern for flow in driven cavity, $\Re = 400$.

FEM code contained the identical set of nodes as the 41x41 vorticity FEM grids. It is interesting to note that the 21x21 vorticity FEM results, which contains approximately 1/4 of the grid points compared to the primitive-variable FEM grid and uses bilinear compared to biquadratic elements, provided more accurate results than the primitive-variable FEM code.

To further show the accuracy of the current approach for solving the vorticity equation, quantitative comparisons are made with the multigrid results for the location and extent of primary and corner vortices in Table 1. The following comparisons are made between the current Dirichlet FEM vorticity solutions using a 41x41 uniform grid and the multigrid finite difference solutions of Ghia *et al.* [8] on a 129x129 grid. As seen in the Table, the comparison between the FEM and FDM results is excellent. It is particularly noteworthy that the solutions using the

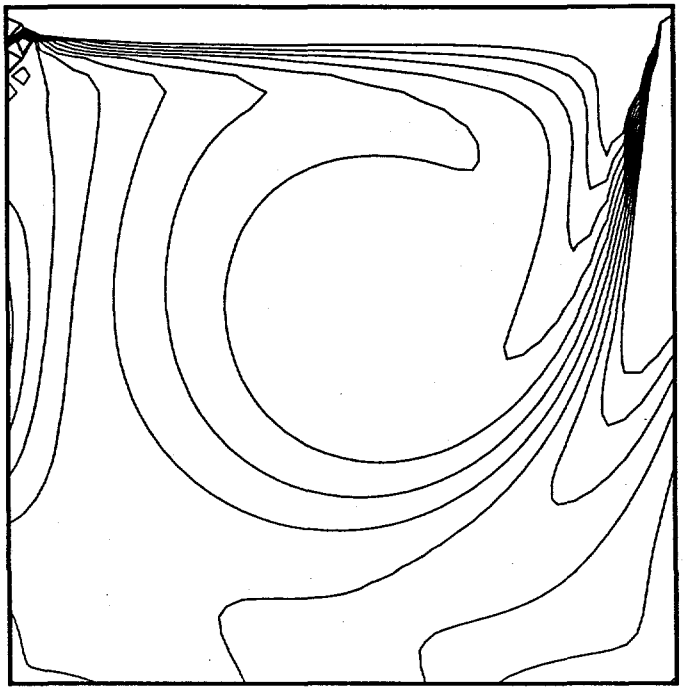

FIG. 7. Vorticity contours for flow in driven cavity, $\Re = 400$.

vorticity formulation are able to provide an excellent resolution of the two bottom secondary vortices on a relatively coarse grid.

The vortex sheet formulation of the GHD yields a Fredholm integral equation of the second kind while the boundary vorticity formulation yields a Fredholm integral equation of the first kind. As discussed above, an LU decomposition is performed outside the time loop. For the 41x41 grid, the condition number for the vortex sheet formulation was 6.68 whereas the condition number for the boundary vorticity formulation was 13.68. Both condition numbers are small for a system of 1681 linear equations. The reason that the first kind formulation yields a small condition number (on the same order as the second kind formulation) is because of the singular nature of the Green's function in the domain integral which results in large diagonal matrix elements.

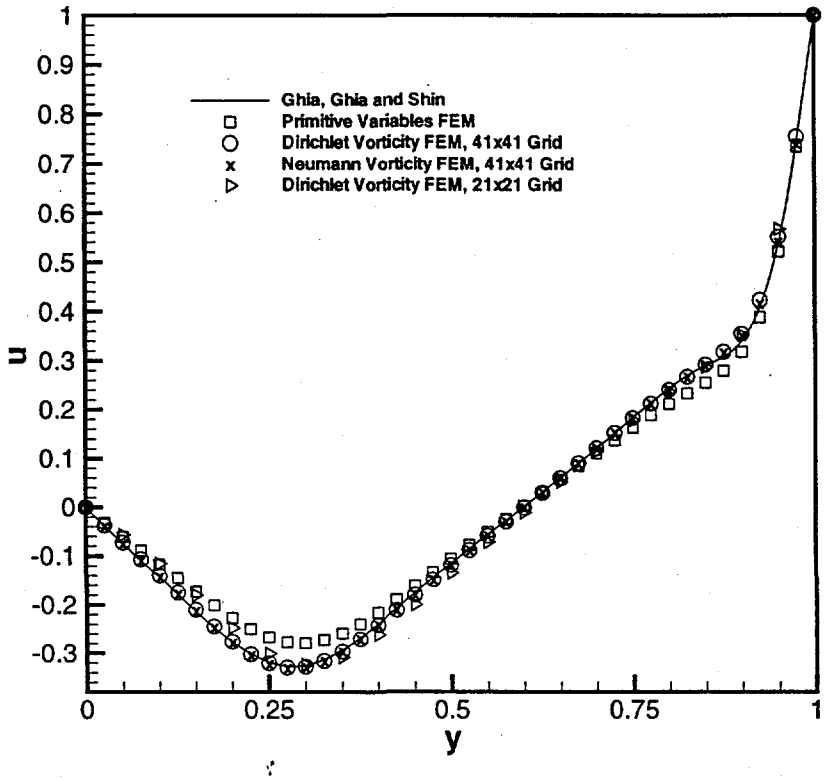

FIG. 8. Steady-state results for u-component of velocity along the vertical line through the geometric center of the cavity.

The results due to Ghia, Ghia, and Shen and the primitive-variable FEM results are steady state solutions. The vorticity FEM results are run through the transient starting with an impulsively-started upper lid. A comparison of the Neumann vorticity FEM and the Dirichlet vorticity FEM is performed for the transient solution. The u-component of velocity is shown in Figure 9 at the point $x = 0.5, y = 0.9$ (the origin is located at the lower left hand corner of the cavity). Although there are some differences between the two methods in the early transient, at the field point $(x = 0.5, y = 0.9)$, the largest discrepancy in the u-component of velocity at the field point after the first second is 0.0041%, the largest discrepancy in the v-component of velocity is 0.0013%, and the largest discrepancy in the vorticity is 0.0085%. Further, for more realistic situations in which the initial and boundary

TABLE 1
Comparison of primary and secondary vortex data between Dirichlet FEM vorticity solution and primitive variable FDM solution of Ghia *et al.* [8].

	Dirichlet FEM Results	Multigrid FDM Results
(x,y) coordinates of primary vortex	(0.5535,0.6066)	(0.5547,0.6055)
Length of bottom left vortex on lower wall	0.1098	0.1081
Height of bottom left vortex along side wall	0.1312	0.1273
Length of bottom right vortex on lower wall	0.2676	0.2617
Height of bottom right vortex along side wall	0.3272	0.3203

data are not discontinuous, this level of agreement between the two methods could be expected even in the very early transient.

Finally as discussed in subsection 3.2, the accuracy of the numerical quadratures used in the discretized Galerkin GHD can be assessed by taking column sums of the associated linear system of equations. Analytic values for the column sums can be determined for the Dirichlet problem from Eq. 31 and for the Neumann problem from Eq. 29. For the Dirichlet problem on the uniform 21x21 grid, the analytic column sum is given by $\pi/800$ for finite element nodal basis functions associated with corner nodes and $\pi/400$ for finite element nodal basis functions associated with edge nodes. The calculated column sums for finite element nodal basis functions associated with corner nodes agreed to 14 significant figures. The result to 6 significant figures is given by 3.92732E-3 which shows a relative error of 8.4599E-5 compared to the analytic value. The calculated column sums for nodal basis functions associated with edge nodes agreed to 6 significant figures given by 7.85397E-3 which shows a relative error of 1.2528E-6. For the Neumann

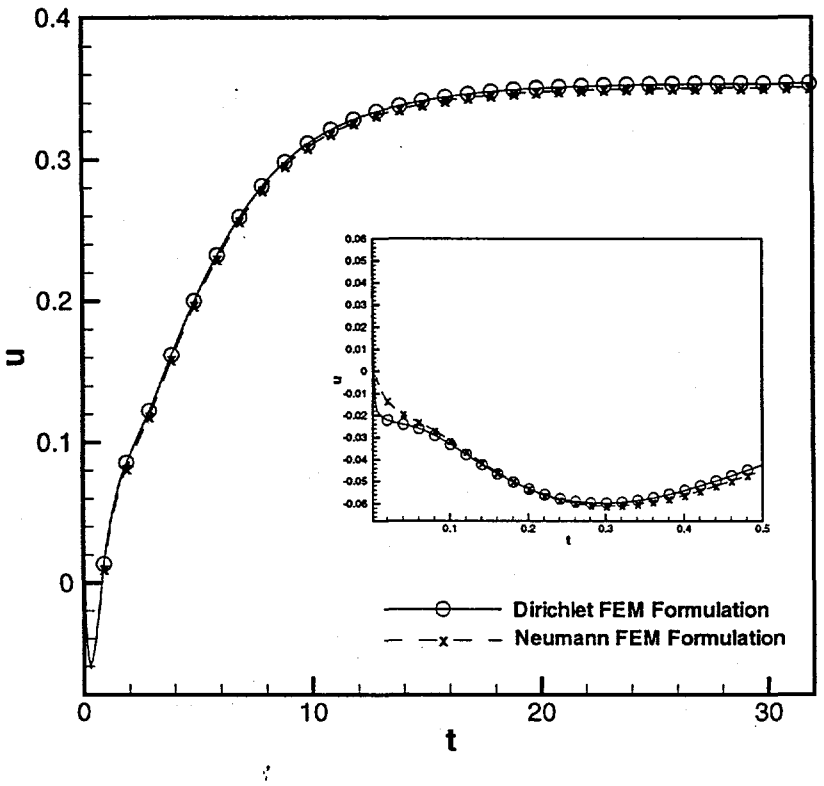

FIG. 9. Transient results for the u-component of velocity at the point $x = 0.5, y = 0.9$. The inset is a blow-up of the plot for early times.

problem on the uniform 21x21 grid, the analytic column sum is given by $\pi/20$ for all boundary element nodal basis functions associated with corner nodes and $\pi/10$ for all other boundary element nodal basis functions. The calculated column sums for the boundary element nodal basis functions associated with corner nodes agreed to 14 significant figures. The result to 6 significant figures is given by 0.157182 which shows a relative error of 6.5165E-4 with the analytic value. The calculated column sums for all other boundary element nodal basis functions agreed to 11 significant figures. This result to 6 significant figures is given by 0.314159 which shows a relative error of 2.7827E-8. These calculated column sums demonstrate the accuracy with which both the domain and boundary integrals are performed in the Galerkin GHD.

5. CONCLUSIONS

Two approaches for determining boundary conditions appropriate for the vorticity form of the Navier-Stokes equations are presented in this research. Both approaches are based on a Galerkin implementation for the generalized Helmholtz decomposition (GHD). There are several advantages both numerically and conceptually in using a Galerkin formulation as opposed to the more traditional point-collocation formulations.

The accuracy of the Galerkin formulation is shown to be far more accurate than the point-collocation formulation. Many researchers in the past have added constraint equations when attempting to implement the GHD to solve for vortex sheet strengths. It is possible that a constraint such as imposing Stokes theorem was necessary for point-collocation methods in order that excess vorticity not accumulate within the domain over time because of poorly approximated vorticity creation on the boundary. No constraint equations are implemented in the current formulation.

There has been considerable debate in the literature concerning which component of the GHD should be imposed in order to satisfy the velocity boundary conditions. The conceptual advantage of the Galerkin formulation is that it can be proven that the normal component leads to a rank-deficient set of linear equations. Further, the tangential component leads to an integral constraint that is implicitly satisfied by the GHD. This constraint equation can be related to column sums associated with the linear equations which can be used to test the accuracy of the integral evaluations of the GHD. Although the tangential component of the GHD is used by necessity to determine either boundary vorticity or vortex sheet strengths, the level of accuracy in satisfying the velocity boundary conditions in the tangential and normal directions are of the same order of magnitude.

There is extra computational expense in implementing the Galerkin formulation of the GHD compared to the point-collocation formulation. However, this computational expense is performed only once outside the time loop. Further, it is quite likely that the Galerkin formulation would actually be less expensive for a comparable level of accuracy.

There has also been some debate in the literature whether it was more appropriate to determine boundary vorticity yielding Dirichlet boundary conditions or determine vortex sheet strengths yielding Neumann boundary conditions. A direct comparison is performed in this research (perhaps for the first time) showing that the two approaches are essentially equivalent yielding numerical results that are typically only a fraction of a percent apart. Solving for boundary vorticity results in a Fredholm integral equation of the first kind whereas solving for vortex sheet strengths results in a Fredholm integral equation of the second kind. Typically, Fredholm integral equations of the second kind result in more stable numerical methods characterized by well-conditioned discretized linear systems. However, in the case of the GHD because of the singular nature of the domain integrand, both approaches yield very well conditioned discretized linear equations.

A Galerkin finite element method is implemented to solve the vorticity equation using the GHD to provide appropriate boundary conditions as discussed above. The vorticity equation is linearized again using the GHD to determine the interior velocities. The driven cavity problem at a Reynolds number of 400 is considered as a benchmark. Both vorticity formulations (Neumann and Dirichlet) are shown to provide more accurate results than a primitive variable formulation for the same level of discretization. In fact, the vorticity formulations using 1681 grid points compared very favorably to a multigrid finite difference method using 16,641 grid points.

ACKNOWLEDGMENT

This work was supported by Sandia National Laboratories, a multiprogram laboratory operated by Sandia Corporation, a Lockheed-Martin Company, for the U.S. Department of Energy under Contract DE-AC04-94AL85000.

REFERENCES

1. Anderson, C. R., Vorticity boundary conditions and boundary vorticity generation for two-dimensional viscous incompressible flow, *J. Comput. Phys.* **80**, 72 (1989).

2. Batchelor, G. K., *An Introduction to Fluid Mechanics* (Cambridge University Press, 1967).

3. Bykhovskiy, E. B. and N. V. Smirnov, On orthogonal expansions of the space of vector functions which are square-summable over a given domain and the vector analysis operators, NASA TM-77051 (1983).

4. Chorin, A. J. and J. E. Marsden, *A Mathematical Introduction to Fluid Mechanics*, Second Edition (Springer-Verlag, Berlin, 1990).

5. Daube, O., Resolution of the 2D Navier-Stokes equations in velocity-vorticity form by means of an influence matrix, *J. Comput. Phys.* **103**, 402 (1992).

6. Brebbia, C. A. and J. Dominguez, *Boundary Elements Elements. An Introductory Course*, (McGraw-Hill, New York, 1989).

7. Gatski, T. B., C. E. Grosch, and M. E. Rose, The numerical solution of the Navier-Stokes equations for 3-dimensional, unsteady, incompressible flows by compact scheme, *J. Fluid Mech.* **82**, 298 (1989).

8. Ghia, U., Ghia, K. N., and Shin, C. T., High-Re solutions for incompressible flow using the Navier-Stokes equations and a multigrid method, *J. Comp. Phys.* **48**, 387 (1982).

9. Gresho, P. M., Incompressible fluid dynamics: Some fundamental formulation issues, *Ann. Rev. Fluid Mech.* **23**, 413 (1991).

10. Hribersek, M. and Skerget, L., Iterative methods in solving Navier-Stokes equations by the boundary element method, *Int. J. Num. Meth. Engrg.* **39**, 115 (1996).

11. Kempka, S. N., Glass, M. W., Strickland, J. H., and Ingber, M. S., Accuracy considerations for implementing velocity boundary conditions in vorticity formulations, Sandia National Laboratories Report SAND96-0583, Albuquerque, NM, (1996).

12. Kinney, R. B. and M. A. Paolino, Flow transient near the leading edge of a flat plate moving through a viscous fluid, *ASME J. Appl. Mech.* **41**, 919 (1974).

13. Koumoutsakos, P., A. Leonard, and F. Pepin, Boundary conditions for viscous vortex methods, *J. Comput. Phys.* **113**, 52 (1994).

14. Leonard, A., Vortex methods for flow simulation, *J. Comput. Phys.* **37**, 289 (1980).

15. Leonard, A., Computing three-dimensional incompressible flow with vortex elements, *Ann. Rev. Fluid Mech.* **17**, 523 (1985).

16. Lighthill, M. J., Chapter II. Introduction: Boundary Layer Theory, in *Laminar Boundary Layers*, Rosenhead, L., Editor, (Clarendon Press 1963).

17. Meir, A. J. and P. G. Schmidt, Variational methods for stationary MHP flow under natural interface conditions, *J. Nonlin. Anal.* **26**(4), 659 (1996).

18. Morino, L., Helmholtz decomposition revisitied: Vorticity generation and trailing edge condition, *Comput. Mech.* **1**, 65 (1986).

19. Morino, L., Boundary integral equations in aerodynamics, *Appl. Mech. Rev.* **46**(8), 445 (1993).

20. Morse, P. M. and H. Feshback, *Methods of Theoretical Physics*, Part II, (McGraw-Hill, New York, 1953).

21. Ostrikov, N. N. and E. M. Zhmulin, Vortex dynamics of viscous fluid flows: Part 1. Two-dimensional flows, *J. Fl. Mech.* **276**, 81 (1994).

22. Parmentier, E. M. and K. E. Torrance, Kinematically consistent velocity fields for hydrodynamic calculations in curvilinear coordinates, *J. Comput. Phys.* **19**, 404 (1975).

23. Puckett, E. G., Vortex methods: An introduction and survey of selected research topics, in *Incompressible Computational Fluid Dynamics*, edited by Gunzburger, M. D. and R. A. Nicolaides (Cambridge University Press 1993).

24. Quartapelle, L., Vorticity conditioning in the computation of two-dimensional viscous flows, *J. Comput. Phys.* **40**, 453 (1981).

25. Quartapelle, L. and F. Valz-Gris, Projection conditions on the vorticity in viscous incompressible flows, *Int. J. Num. Meths. Fluids* **1**, 129 (1981).

26. Roache, P., Computational Fluid Dynamics, Hermosa Press, Albuquerque, NM, 1972.

27. Sarpkaya, T., Vortex element methods for flow simulation, *Adv. Appl. Mech.* **31**, 113 (1994).

28. Uhlman, J. S. and J. Grant, A new method for implementation of boundary conditions in the discrete vortex element method, ASME Fluids Engrg. Sprg. Mtg., Washington, D.C., 1993.

29. Wu, J. C. and J. F. Thompson, Numerical solutions of time-dependent incompressible Navier-Stokes equations using an integro-differential formulation, *Comput. Fluids* **1**, 197 (1973).

30. Wu, J. C., Numerical boundary conditions for viscous flow problems, *AIAA J.* **14**, 1042 (1976).

31. Wu, J. C. and U. Gulcat, Separate treatment of attached and detached flow regions in general viscous flows, *AIAA J.* **19**(1), 20 (1981).

32. Wu, J. C., Boundary elements and viscous flows, in Boundary Element Technology VII, Brebbia, C. A. and M. S. Ingber, Eds., 3-18, (Elsevier Applied Science, Amsterdam, 1992).

33. Wu, J. Z., X. Wu, H. Ma, and J. Wu, Dynamic vorticity condition: Theoretical analysis and numerical implementation, *Int. J. Num Meths. Fluids* **19**, 905 (1994).